

Video Article

# Cortical Source Analysis of High-Density EEG Recordings in Children

Joe Bathelt<sup>1</sup>, Helen O'Reilly<sup>2</sup>, Michelle de Haan<sup>1</sup>

<sup>1</sup>Cognitive Neuroscience & Neuropsychiatry Section, UCL Institute of Child Health

<sup>2</sup>Academic Division of Neonatology, Institute for Women's Health, University College London

Correspondence to: Joe Bathelt at [johannes.bathelt.10@ucl.ac.uk](mailto:johannes.bathelt.10@ucl.ac.uk)

URL: <http://www.jove.com/video/51705>

DOI: [doi:10.3791/51705](https://doi.org/10.3791/51705)

Keywords: Behavior, Issue 88, EEG, electroencephalogram, development, source analysis, pediatric, minimum-norm estimation, cognitive neuroscience, event-related potentials

Date Published: 6/30/2014

Citation: Bathelt, J., O'Reilly, H., de Haan, M. Cortical Source Analysis of High-Density EEG Recordings in Children. *J. Vis. Exp.* (88), e51705, doi:10.3791/51705 (2014).

## Abstract

EEG is traditionally described as a neuroimaging technique with high temporal and low spatial resolution. Recent advances in biophysical modelling and signal processing make it possible to exploit information from other imaging modalities like structural MRI that provide high spatial resolution to overcome this constraint<sup>1</sup>. This is especially useful for investigations that require high resolution in the temporal as well as spatial domain. In addition, due to the easy application and low cost of EEG recordings, EEG is often the method of choice when working with populations, such as young children, that do not tolerate functional MRI scans well. However, in order to investigate which neural substrates are involved, anatomical information from structural MRI is still needed. Most EEG analysis packages work with standard head models that are based on adult anatomy. The accuracy of these models when used for children is limited<sup>2</sup>, because the composition and spatial configuration of head tissues changes dramatically over development<sup>3</sup>.

In the present paper, we provide an overview of our recent work in utilizing head models based on individual structural MRI scans or age specific head models to reconstruct the cortical generators of high density EEG. This article describes how EEG recordings are acquired, processed, and analyzed with pediatric populations at the London Baby Lab, including laboratory setup, task design, EEG preprocessing, MRI processing, and EEG channel level and source analysis.

## Video Link

The video component of this article can be found at <http://www.jove.com/video/51705/>

## Introduction

President Barack Obama described the human brain as the next frontier of scientific discovery with high importance for health and economy<sup>3</sup> (<http://www.whitehouse.gov/share/brain-initiative>). However, like any other field in the natural sciences, neuroscience depends on advances in methodologies and analysis techniques for progress. Two commonly used non invasive tools in studies about brain function in humans are magnetic resonance imaging (MRI) and electroencephalography (EEG). These tool exploit different physical properties and provide different insights into brain function with unique advantages and disadvantages. MRI uses the magnetic properties of water molecules within magnetic fields to obtain images of living tissues. The subject needs to be placed in a magnet with high field strength. The participant's movement is restricted during this procedures and the participant has to tolerate noise caused by rapid changes in the magnetic field. In addition to structural images, MRI also provides the possibility to measure changes in blood oxygenation to investigate brain function (fMRI). In summary, MRI offers relatively high spatial resolution of up to 0.5 mm<sup>3</sup> with modern high fields scanners and optimized parameters<sup>4</sup>. In contrast, the temporal resolution of fMRI is limited to the slow kinetics of the BOLD response, which only indirectly reflects the high temporal dynamics of neural activity<sup>5,6</sup>.

On the other hand, EEG measures changes in electrical activity caused by the activity of neurons through electrodes placed on the scalp. Recent advances in EEG technology allow quick and easy application of the sensors for short term or long term and stationary as well as ambulatory recordings. Because EEG is less restrictive, it is also the method of choice for certain participant populations that do not tolerate the MRI environment well like pediatric and certain geriatric and psychiatric populations. The properties of EEG show an inverse pattern to those of MRI: the temporal resolution is very high with millisecond precision, but the spatial resolution is limited. Electrical currents pass through different tissues between their generator and the EEG electrodes on the surface of the scalp. This leads to mixing and spatial smearing of source activity known as the volume conduction effect. Therefore, activity measured by the electrodes on the surface of the scalp reflects activity from multiple sources that might be distant to the position of the electrode on the head<sup>1,7</sup>.

Much work in recent years has been dedicated to the merging of MRI and EEG in order to take advantage of their respective strengths. One line of work is dedicated to the simultaneous acquisition of EEG and MRI in functional studies. Another approach is to use the spatial information provided by structural MRI to take account of the volume conduction effect through biophysical modelling. The use of structural information for

source reconstruction of EEG recordings is particularly useful for studies involving a pediatric population. The investigation of the development of brain function is central to understanding how complex cognitive skills are built on top of simple precursors<sup>8</sup>.

These investigations help to highlight changes in the neural substrates and response properties that correlate with changes in behavioral performance. However, the investigation of brain function and cognition during development also poses specific challenges. Particularly, the opportunity for functional MRI studies is limited as young children and infants either have to be asleep or sedated to obtain MRI data without movement artifacts and negative impact on participant wellbeing. Further, EEG is perceived as less risky and invasive by parents, which makes the recruitment of research participants easier. Therefore, EEG is the method of choice for many investigations of brain function in young children. Methodological advances in EEG systems allow the application of high density electrode arrays with 128 or more channels within minutes. Ease of application and wearing comfort are sufficient to even allow EEG recording in the youngest infants. However, often researchers are not only interested in the temporal dynamics of responses to particular stimuli, but would also like to compare the neural substrates that mediate the responses.

A prevailing assumption in channel level ERP analysis comparing different age groups is that the same neural substrates respond, but that the timing or response amplitude varies across ages<sup>9</sup>. Similar scalp topography is often used as an indicator of similar underlying neural activity. However, many different source configurations can lead to similar scalp topographies<sup>10</sup>. By applying source estimation, this uncertainty can be reduced and quantified. The independence of observations is critical for network accounts of brain function: if the sources are mixed, correlations will be biased towards higher local connectivity. Source reconstruction can be applied to reduce this bias<sup>11</sup>. Alternatively, differences in timing and phase can be used for connectivity analysis, but these mathematical models require assumptions that are hard to evaluate in non simulated data<sup>12</sup>. In summary, source estimation provides additional information to channel level EEG and ERP analysis based on knowledge about anatomy and biophysical properties of tissue.

Different algorithms have been devised to find solutions to the inverse problem. These algorithms fall broadly into two categories: parametric and non parametric<sup>13</sup>. Parametric models assume one or multiple dipoles that may vary in location, orientation and strength. In contrast, non parametric models contain a large number of dipoles with fixed location and orientation. In these models, the scalp electrical activity is explained as a combination of activations in the fixed dipoles<sup>10,13,14</sup>. Non parametric, distributed source models can be based on knowledge about anatomy and conductivity in different media. Boundary Element Models incorporate conductivity values for the main tissues of the head with different shells for the brain, cerebro spinal fluid, and skull. This is based on the assumption that conductivity is mostly constant within each compartment, but that marked changes occur at the boundary of different compartments. Finite element models are based on further segmentation of MR scans into grey and white matter so that conductivity values can be assigned to each voxel<sup>15</sup>.

In practical terms, non parametric models are particularly useful for source reconstruction in complex cognitive tasks, in which the number of areas involved may not be known<sup>10</sup>. Boundary element models are most widely used in the current literature, probably because the more accurate Finite Element Models pose comparably high computational demands. Further, there is considerable inter individual variability in grey and white matter so that FEMs should be based on individual MRI scans.

Non parametric models require a second step for matching the scalp measured activity to the predictions of the forward model. Again, different approaches with different advantages and drawbacks have been discussed in the literature (see Michel *et al.* 2004 for an overview). The most widely used algorithms are based on minimum norm estimation (MNE), which matches the scalp measured activity to a current distribution in the forward model with the lowest overall intensity<sup>16</sup>. MNE is biased towards weak and superficial sources. Depth weighted MNE algorithms try to reduce the surface bias by introducing weighting matrices based on mathematical assumptions<sup>10</sup>. The widely used LORETA approach is also based on weighted MNE, but additionally minimizes the Laplacian of sources, which leads to smoother solutions<sup>17,18</sup>. LORETA has been found to perform best for single sources in simulation studies<sup>19,20</sup>. However, LORETA may lead to over smoothing of solutions. Depth weighted MNE is preferable when the sources are unknown or multiple sources are likely to be present<sup>13,16</sup>. Comparing the results of different algorithms to evaluate the influence of different model assumptions is recommended.

In summary, source reconstruction through modelling methods has been limited for children until recently. This is because most EEG analysis software relies on head models based on adult anatomy that substantially limits the accuracy of source solutions in children<sup>2,8</sup>. The cheap access to computational power and the provision of user friendly software for source reconstruction make it possible to overcome these limitations. Applying source estimation to the EEG provides two important advantages over analysis based on channel level observations alone: improved spatial resolution and independence of observations.

Source estimation may not be informative in some cases: good coverage of the head is required to distinguish sources. High density systems with 128 or more electrodes are recommended<sup>10,15</sup>; a sparser coverage will act as a spatial filter leading to more wide spread source activation or false negative results<sup>10</sup>. Furthermore, source reconstruction based on the method described in this article has only been reported for cortical generators. Therefore, it is less suitable for testing hypotheses about subcortical substrates or cortical subcortical interactions. Lastly, source analysis should be based on detailed prior hypotheses about the cortical substrates, taking the existing literature from other imaging modalities into account. Spatial filtering techniques may also be used to improve the spatial resolution of the EEG signal by reducing spatial mixing on the scalp level. Alternative methods to reduce the influence of volume conduction effects without head modelling are used, e.g., Laplacian filtering<sup>21</sup> or Current Source Density analysis<sup>22</sup>. However, these methods do not provide more information about neural generators as volume conduction effects are not only restricted to sensors in close spatial proximity<sup>1</sup>.

In the following sections, the article describes how experiments for the investigation of brain and cognitive function in children from 2 years of age are designed at the London Baby Lab. Next, EEG data acquisition with high density low impedance systems with children is discussed. Then, EEG preprocessing and analysis on the channel level is presented. Lastly, the article focuses on the processing of structural MRI data for cortical source reconstruction and analysis of source level signals.

## Protocol

### 1. Designing EEG & Event related potential experiments for children

Note: A simple experiment was designed for the purposes of this article that may be used to investigate face processing in young children. The following section will describe the experiment and explain how to implement it using MATLAB R2012b and Psychtoolbox V3.0.11<sup>23,24</sup>. Pictures taken from the NimStim set of emotional facial expression<sup>25</sup> were used for this example. This stimulus set is available for research purposes upon request (<http://www.macbrain.org/resources.htm>).

1. Transfer the RGB pictures to grey scale to reduce differences between stimuli. See **Table 1**. Note: These commands require the Image Processing Toolbox (<http://www.mathworks.co.uk/products/image/>). Free alternatives may be found through the File Exchange (<https://www.mathworks.co.uk/matlabcentral/fileexchange>).
2. Use experimental control software to implement the experiment with precise timing for stimulus presentation triggers using a series of commands (see **Table 1** for an example).

### 2. Data Acquisition

1. Ensure that the child is comfortable with the testing environment. Allow younger children to sit on the lap of their caregiver or in a comfortable child's seat. Let the child see and feel the sensor net before applying it to the child's head. If there is an extra net, have the parent also try one on, or place one on a doll or stuffed teddy.
2. Measure the maximum head circumference to select the correct net size for the child. Use a measuring tape and hold it to the nasion. Then measure around the head around the maximum circumference (~1 cm above the inion). Note: keep a record of the measured head circumference and the sensor net used for later analysis<sup>26</sup>. It helps if the parents head is also measured to make children more comfortable with the situation.
3. Identify the vertex of the head at the intersection of the mid distance between nasion and inion and left and right periauricular point. Mark this point with a china pen to ensure that the vertex channel is correctly positioned when applying the net.
4. Apply the sensor net and make sure that key channels are aligned with the anatomical landmarks (nasion, inion, vertex and left/right mastoids). Note: For the most accurate results, the position of the channels on the head can be digitally acquired using special digitization equipment. Researchers wishing to acquire the sensor position should refer to the appropriate hardware and software manuals. Alternatively, electrode maps that assume standard placement of electrodes along anatomical landmarks can be used. These maps can be warped to age appropriate head models as described in the analysis section.
5. Ensure that channels have good contact with the scalp by positioning the sensors individually; gently twist each sensor from side to side to move hair out of the way.
6. Measure channel gains and channel impedances. Click "Start" to begin the recording in NetStation EEG recording software and start gain and impedance measurement. If measurement does not automatically start, use the "Calibrate Amplifier" and the "Measure Net Impedances" button.
7. Check the recording software for channels with impedances higher than 50 k $\Omega$  which will appear red. Apply additional electrolyte solution with a pipette to lower channel impedances. Check the EEG display for channels that show high frequency activity despite low impedance or noticeably less activity than surrounding channels (flat line channels). These channels may have loose contact with the scalp and require adjustment.
8. In order to keep children comfortable during the EEG preparation, allow the child to listen to music, watch an age appropriate cartoon or distract them using another experimenter, e.g., blowing soap bubbles for toddlers.

### 3. Analysis

1. Preprocessing
  1. Digitally filter the data with a high pass filter with a cut off at 0.1 Hz to remove channel drifts<sup>27</sup> (**Table 1**).
  2. For ERP analysis, apply a low pass filter with a cut off at 30 Hz<sup>27</sup> (**Table 1**).
  3. Epoch the continuous data according to the trigger codes set during recording. For most experiments, use a baseline of 200 msec prior to stimulus onset and a post stimulus interval of 600 msec to cover the time interval of interest (**Table 1**).
  4. Remove epochs that contain movement or blink artifacts: mark channels with a peak to peak amplitude higher than 150 mV - adjust this threshold depending on the participant group and data quality. For consistency, use the same threshold for all participants in one study. If a channel is above this threshold in more than 30% of the epochs, remove the channel (channel activity may be interpolated from surrounding channels, if these contain acceptable data). If more than 20% of the channels are marked as bad in an epoch, remove the epoch. If more than 20% of channels are rejected by the algorithm or less than 50% of epochs are retained, consider removing the dataset from further analysis (**Table 1**).  
Note: The percentage thresholds for epoch and channel rejection are ballpark figures that remove a sufficient amount of noise in our experience. The amount of artifact in the recording is likely to be different using other participant groups, experimental paradigms or EEG systems. The experimenters may want to adjust the percentage thresholds and check if they are satisfied with the artifact rejection. Alternatively, experimenters can reject trials that contain artifact through visual inspection.
  5. Re reference to average reference by subtracting the mean activity across channels from each channel (**Table 1**). Note: The vertex electrode is typically used as the recording reference in NetStation.
2. Artifact Correction Using Independent Component Analysis
  1. Import the data into the FASTER toolbox<sup>28</sup> and run the automatic artifact rejection algorithm on the data (**Table 1**).
  2. Use the Graphical User Interface (GUI) for FASTER; to open the GUI, type FASTER\_GUI into the command line.

3. Deselect the filtering options in the filtering menu as the data has already been filtered before the epoching.
  4. Specify the number of channels: 126 EEG channels with 2 electrooculogram (EOG) channels.
  5. Enter the markers used for epoching the data as strings in a cell array. For the presented case enter: {'face', 'scra'} for the face and scrambled face conditions.
  6. Select the channels for the independent component analysis (ICA). Typically select all recording channels, incl. external non EEG channels.
  7. Specify the input and output folder in the right pane of the GUI.
  8. Select the appropriate channel file for the recordings. Note: Channel files for most EEG system can either be downloaded from the manufacturer or can be downloaded from the EEGLAB website.
  9. Click RUN to start FASTER processing. Depending on the length of the recordings and the number of files, this processing can take several hours.
  10. Visually inspect the recordings, independent component maps and ERPs after the processing.
3. Channel Level Analysis of Event-related Potentials Data
    1. Combine several channels to form a virtual channel with better signal to noise ratio (**Table 1**). Note: The selection of channels should be based on previous reports in the literature or *a priori* hypotheses. Selecting channels that show the highest amplitude within a given time window is not advised<sup>29</sup>.
    2. Obtain measures like peak amplitude, mean amplitude and peak latency to characterize the waveform and perform statistical tests (**Table 1**).
  4. Create Boundary Element Models (BEM)
    1. Segment the anatomical MRI scan with FreeSurfer. Note: For the most accurate results, base the boundary element model on individual MRI scans for each participant. If this is not feasible, average MRI templates that match the participants' age as closely as possible should be used. Please note that BEMs cannot be used for children under 24 months. Boundary element models assume that each shell (brain, skull, skin) consists of a closed shell. However, in young children the fontanelles in the skull are not closed, which violates the closed shell assumption.
      1. In order to install FreeSurfer software, first download it from the FreeSurfer website (<http://freesurfer.net/fswiki/DownloadAndInstall>). Next, set up the shell environment include FreeSurfer; for .bashrc, include the following commands in the .bashrc file:
        1. Export FREESURFER\_HOME=/Applications/freesurfer/
        2. Source \$FREESURFER\_HOME/FreeSurferEnv.sh
 Note: These commands assume that the FreeSurfer folder is in the Applications folder on a Unix system. There are more details on how to setup FreeSurfer with alternative shell environments, e.g. csh/tcsh, or operating systems on the FreeSurfer website (<http://freesurfer.net/fswiki/DownloadAndInstall>).
      2. Next, define the Subject directory, i.e. the folder that the output will be written to using the following command:
        1. export SUBJECTS\_DIR=../BEMs/
 Note: The results may be written to any folder on the system.
      3. Next, change the working directory to the folder that contains the MRI file for the Boundary Element Model using the following command:
        1. cd /Users/joebathelt/Neurodevelopmental\_MRI\_database/Children/Brain/
 Note: Any folder on the system may be specified using the syntax of the cd command. This is an example of the primary researchers file structure.
      4. Finally, start the reconstruction using the following commands:
        1. recon-all -i <mri\_file> -subjid <subject\_id>
        2. recon-all -all -subjid <subject\_id>
 Note: <mri\_file> needs to be replaced with the filename of the desired MRI scans in the current directory. <subject\_id> can be replaced with any name. FreeSurfer will create a folder with this name in the subject directory. Depending on the system used, the last commands may require some time to run.
    2. Check the FreeSurfer segmentation for incorrect segmentation, e.g. overlapping spheres, anatomically unlikely compartments *etc.* by importing the segments into BrainStorm and use the display tools in the GUI:
      1. In BrainStorm, select the anatomy pane. Import the segmented MRI by right clicking on the subject and selecting "Import Anatomy Folder". Ensure the folder with the FreeSurfer output is selected. Inspect the segmentation visually by right clicking and selecting "Display". Note: Alternatively, FreeSurfer commands can be used. A detailed description can be found on the FreeSurfer website: <http://surfer.nmr.mgh.harvard.edu/fswiki/RecommendedReconstruction>. If region of interest analysis based on anatomical parcellation is desired, the FreeSurfer functions `mris_ca_label`, `mri_annotation2label` and `mri_mergelabels` can be used. Refer to the FreeSurfer publications and online help pages for more detailed information.
  5. Estimate the Source Activity in BrainStorm
    1. Start BrainStorm by typing "brainstorm" in the command window.
    2. Create a new protocol by selecting New Protocol from the File menu.
    3. Add a new subject to the protocol by selecting New Subject from the File menu.
    4. Import EEG data for the participant by right-clicking on the subject and selecting "Import MEG/EEG".
    5. Import a channel file by right clicking and choosing "Import channel file". Note: The channel file needs to be aligned to the MRI for source reconstruction. BrainStorm uses a system of 4 anatomical reference points that the user needs to mark in the MRI. Please refer to the BrainStorm tutorials for more information (<http://neuroimage.usc.edu/brainstorm/CoordinateSystems>). The standard position as

- defined by a channel file for a certain EEG system or, ideally, the head positions that were digitized prior to the EEG recording can be used.
- Check that the BEM and the channels align as expected: Right click on the channel file for the subject and navigate to "MRI registration" and "Check". Note: If the spheres within the model are overlapping or if the channels are within the BEM, the source reconstruction will produce incorrect results. Adjust the alignment by using the "Edit" option in the "MRI segmentation" menu.
  - Calculate the noise covariance matrix from the baseline of each epoch by right clicking on the participant and choosing "Noise Covariance Matrix" and "Calculate from Recording". Note: The authors of the BrainStorm toolbox recommend using a diagonal noise covariance matrix for short recordings (~ less time points than channels) and a full one for longer recordings. Please refer to the BrainStorm Source Estimation tutorial for more information: <http://neuroimage.usc.edu/brainstorm/Tutorials/TutSourceEstimation>.
  - Calculate the Source Model by right clicking on the subject and selecting "Compute source model".
  - Calculate the inverse solution using depth weighted Minimum Norm Estimation by right clicking on the subject and selecting "Compute Source" and "Minimum norm estimation". Note: Other options (dSPM, sLORETA) are available. Each option has different advantages and drawbacks. The algorithm should be selected based on *a priori* considerations and previous reports in the literature. Further, some algorithms are better in resolving focal activation in certain areas, whereas others are more suitable for wide-spread activation. MNE was used for this study based on previous reports in the literature<sup>16</sup>. For consistency, the same algorithm for inverse solution should be used for all participants in one study. Researchers may also want to compare how robust findings are to the application of different inverse solution algorithms.
  - Repeat Section 3 for all participants in the study. Note: Either use the graphical batching interface or scripts to repeat processing steps for participants. See the BrainStorm documentation for instructions (<http://neuroimage.usc.edu/brainstorm/Tutorials/TutRawScript>).
  - Average source activity over trials per participants by dragging the recordings to the Process Menu and selecting "Average" and "By condition (subject average)".
  - Contrast the condition by selecting the "Processes 2" and dragging each condition in one window. Then, select "Test" and "Student's t-test" or "Student's t-test (paired)" depending on design. To perform multiple comparisons, set amplitude and area thresholds in the display of the resulting statistical map in the "Stat" menu. Note: Alternatively, the activation maps can be exported to SPM (<http://www.fil.ion.ucl.ac.uk/spm/>) for more in-depth statistical analysis (<http://neuroimage.usc.edu/brainstorm/ExportSpm12> HYPERLINK "<http://neuroimage.usc.edu/brainstorm/ExportSpm12>").
  - Calculate the event-related response for a region of interest. For parcellation based ROIs, load the FreeSurfer parcellation by right clicking on the cortex surface in the anatomy menu and select "Import labels". Navigate the corresponding file and load it. Now, select a ROI in the "Scout" pane of the functional data menu.
  - Obtain the ROI event related activity by dragging files to the Process 1 window and select "Extract Scout Time Series" from the Sources menu. Note: Several ROIs can be selected simultaneously and the ROI time series can be exported for further plotting and analysis by right-clicking on the scout time series data and selecting "Export to Matlab".

## Representative Results

Designing ERP experiments for infants and children is often challenging, because of their limited capacity to tolerate long repetitive experiments<sup>30</sup>. This problem is further aggravated when the experimenter plans to apply source reconstruction, because accurate source reconstruction will require a high signal to noise ratio<sup>1</sup>. **Figure 1** displays an experimental protocol for the investigation of face processing mechanisms that can be used with very young children. The paradigm is adapted to a) minimize eye blinks and eye movements during stimulus presentation, because children will be less able to control eye movements than adult volunteers b) make the experiment more engaging by adding attention grabbers after the inter stimulus interval. Eye blinks and eye movements are controlled by presenting a fixation cross shortly before the stimulus in order to draw attention to the center of the screen. Further, the stimulus duration is set to 500 msec, which allows conscious perception of the stimulus while minimizing the time for scanning the image with eye movements. The attention grabber consists of a child friendly image presented with a simultaneous sound. A random selection of different attention grabber stimuli can be used to keep the task interesting for the child. The next trial can be started by the experimenter, when it is clear from the monitoring system that the child is looking at the center of the screen again. In addition, stories can be used to help older children attend to the screen. It is often helpful to practice tasks with children before the EEG recording to make sure that the child understands the task. Screening questions or scores obtained in the practice session can be used as covariates in later analyses.

When calculating the number of repetitions needed for the experiment, it is important to take into account that many trials may be lost due to inattention or movement artifact when working with children. As a rule of thumb, the necessary number of repetitions should be doubled compared to adult studies or recruit a larger number of participants. The attention span and cooperation is limited in children compared to adults. Therefore, keep the specific needs of children in mind when designing the task. A long task can be broken into several blocks of shorter tasks with breaks in between. Typically, the number of conditions that can be included in the experiment is smaller for very young children, as they will not be able to cooperate for the longer periods needed to obtain sufficient trials for many stimulus conditions.

The figures presented are based on a recording with a 6 year old boy (6 years 3 months). The head model was based on an average MRI template of 6 year olds<sup>31</sup>. **Figure 5** shows channel level event related potential responses (ERP) to face and scrambled face stimuli. The waveform of the ERP over posterior channels shows the expected pattern of a positive deflection followed by a negative deflection and a subsequent broad positive deflection. Based on the topography, time course and nature of the paradigm, these deflections are likely to represent the P100, N1 and late positive potential component. Further, the early negative deflection is significantly larger for face stimuli compared to scrambled faces. Therefore, it is likely to reflect the face specific N170 component. The topographic maps in **Figure 5** show the voltage distribution between 250 and 300 msec. Negative voltage with a maximum over right occipito-temporal channels in the faces condition is evident.

**Figure 6** shows the statistical comparison of source activity projected based on a standard adult head model and an age appropriate head model. Source reconstruction was based on a boundary element model (BEM) with depth weighted minimum norm estimation (wMNE) and full noise covariance matrix in Brainstorm v. 3.1<sup>32</sup>. The default MNI Colin27 BEM was used as the adult model. Source activity was averaged over time between 250 and 300 msec in line with face specific responses on the channel level.



The map shows the results of a Student t-test comparison between the faces and scrambled faces condition corrected for multiple comparisons using false discovery rate (FDR). The results show significantly stronger source activation over the temporal lobe in the faces compared to the scrambled faces condition. The localization using the age appropriate model is more focal with strong differences on the ventral surface of the temporal cortex. Localization based on the adult head model is more disperse and shows source activity differences on the right medial and superior temporal gyrus that is mostly absent on the map based on the age appropriate head model.

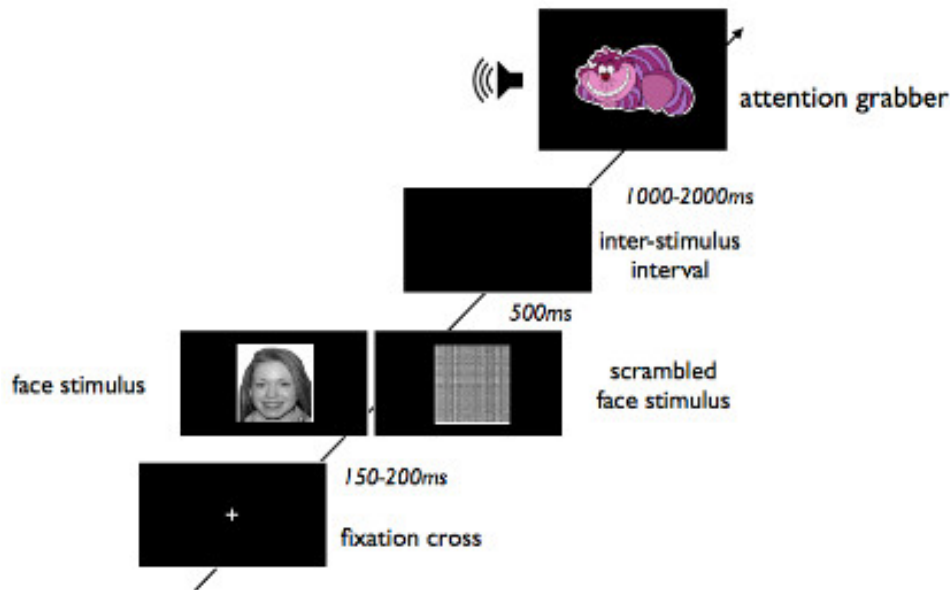


**Figure 1. Example of a face perception experiment suitable over a wide age range** The experiment consists of visual presentation of images of faces or scrambled faces. The stimuli are physically identical, but the spatial arrangement is randomized in the scrambled condition. Each trial begins with central presentation of a fixation cross to minimize eye movements during stimulus presentation. The duration of the fixation cross presentation is randomized to avoid influences of entrainment over multiple repetitions. The stimulus is presented over a duration of 500 msec. The short duration also minimize the chance of eye movements during the presentation window. An attention grabbing stimulus is presented after an inter trial interval with random duration between 1 sec and 2 sec. The attention grabber is particularly useful for very young participants that are not likely to attend to many trials of non engaging material in sequence. The experiment can start the next trial, when the participant is looking on the screen in response to the attention grabber.

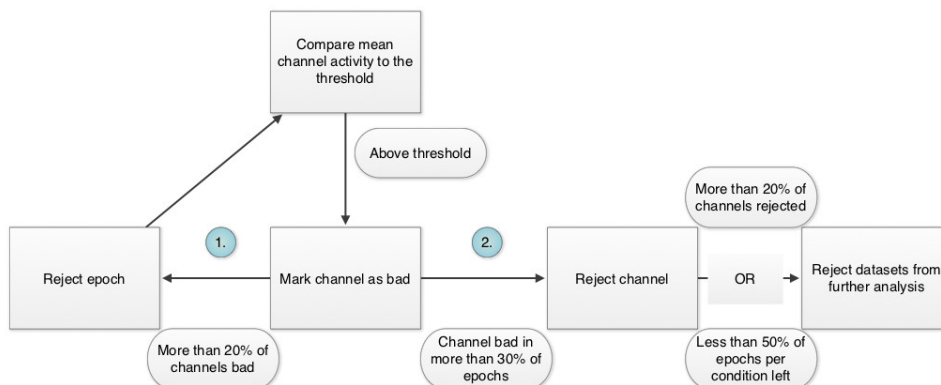


**Figure 2. Flow diagram for the threshold rejection algorithm.** The algorithm compares the maximum of each EEG channel in each epoch to a set threshold. If a channel contains maximum activity above the threshold, the channel is marked as bad. If more than 20% of channels are bad in a given epoch, the epoch is rejected. After epoch rejection, the maximum activity in each channel is compared to the threshold again. If a channel contains activity above the threshold in more than 30% of all epochs, the channel is rejected. If more than 20% of channels are rejected by this procedure or less than 50% of epochs per condition are left after epoch rejection, the dataset should be excluded from further analysis. [Please click here to view a larger version of this figure.](#)

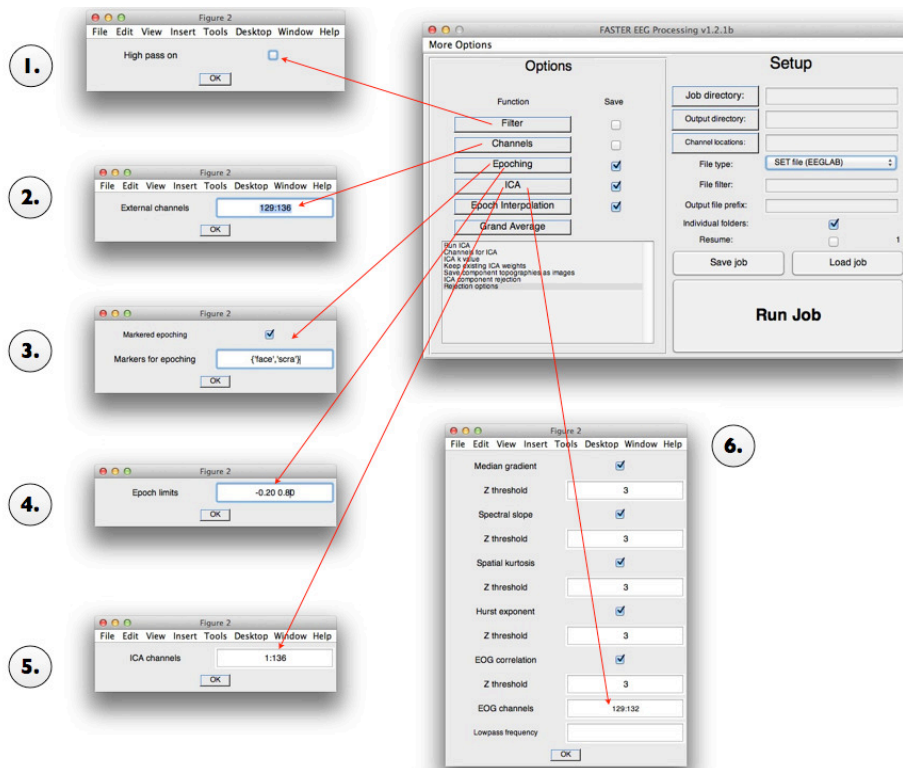


**Figure 3. Automatic artifact correction using the FASTER toolbox<sup>28</sup>**. The figure shows options that need to be changed to use the FASTER toolbox with the setup and processing pipeline described in this article: **1.** Filtering should be disabled, because the dataset has already been filtered **2.** The number of channels needs to be adjusted. The EEG system used in this article has 126 channels with 2 EOG channels. **3.** Event-markers for time locking need to be specified as a cell array of strings. **4.** The time window for the event-related response needs to be supplied. This has to be identical to the window used in the earlier epoching step. **5.** The user has to define channels for the independent component analysis (ICA). In most cases, this would comprise all EEG channels and relevant external channels like the eye channels (EOG). **6.** The indices of the eye channels also need to be adjusted to the EEG system used. For the EEG system described, these would be channels 125 and 128. [Please click here to view a larger version of this figure.](#)

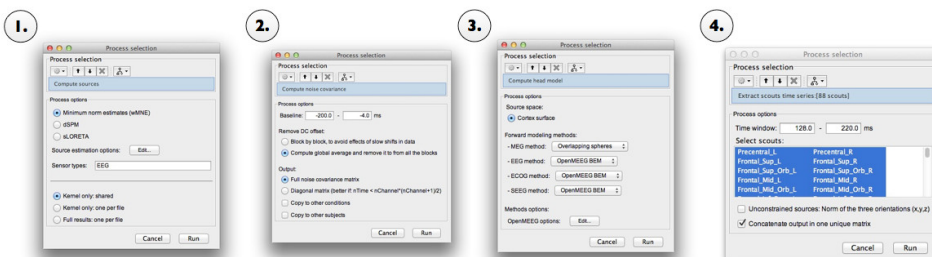


**Figure 4. Source analysis in Brainstorm<sup>32</sup>**. **1.** After importing the EEG dataset and FreeSurfer surfaces, the Boundary Element Model (BEM) can be calculated by selecting "Compute head model" in the "Source" menu. **2.** The noise covariance matrix can be calculated from the recordings by selecting "Compute noise covariance". If the recording is long enough, i.e. more time points than sensors, the full covariance matrix can be computed, otherwise a diagonal matrix is recommended. **3.** After computing the head model and noise covariance matrix, it is possible to obtain the inverse solution. Different algorithms may be used. The depth weighted Minimum Norm Estimation (wMNE) algorithm was used for this article. **4.** The time course of source activity in regions of interest (ROI) can be extracted, by selecting "Extract Scout Time Series" from the "Source" menu. ROIs from automatic cortical parcellation in FreeSurfer were used for this example. [Please click here to view a larger version of this figure.](#)

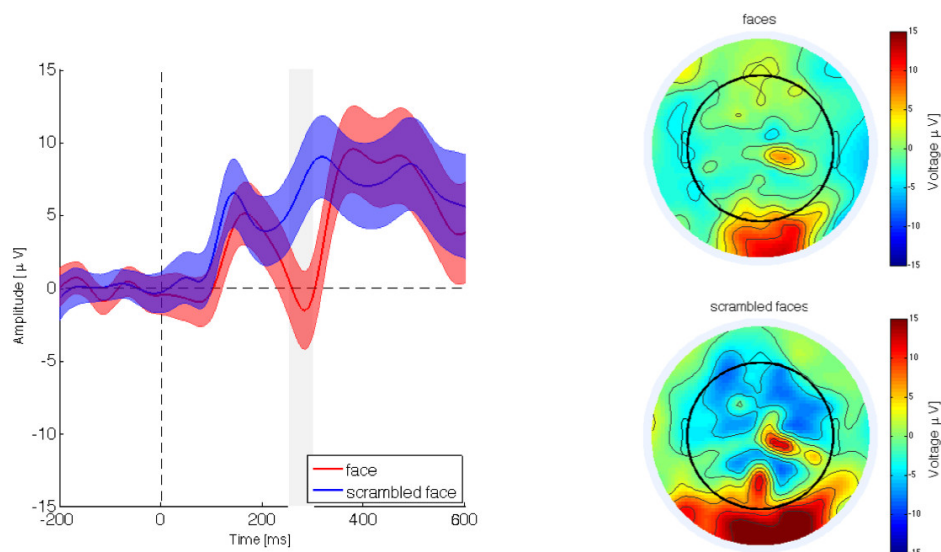


**Figure 5. Event related potentials response (ERP) to face and scrambled face stimuli over right occipito temporal channels.** The ERP shows a more negative deflection between 130 and 220 msec after stimulus onset on the right side for faces compared to scrambled faces. These properties are in line with previous reports about the N170 component<sup>33</sup>. [Please click here to view a larger version of this figure.](#)

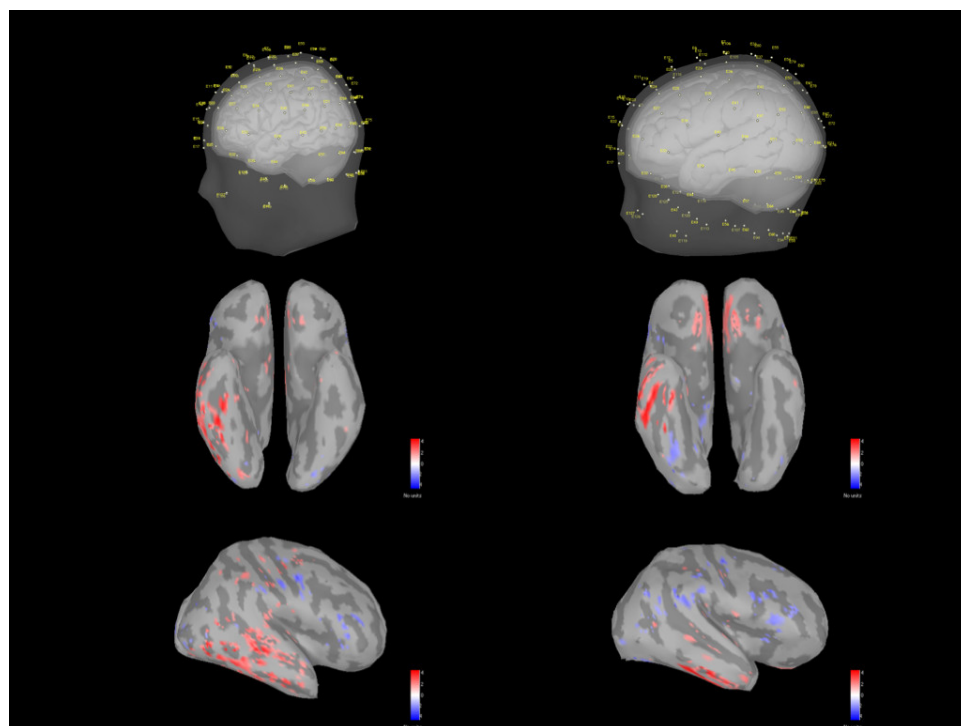


**Figure 6. Comparison of source localization between a default adult head model and an appropriate head model.** The top row of the figure shows the MNI adult boundary head model colin27 on the left and an age appropriate head model based on a FreeSurfer parcellation of an average MRI template for 6 year-old children on the right. The locations of coregistered electrode locations are also presented. The recording was obtained from a 6 year old boy (6 years 3 months). The second and third row show results of a statistical comparison between activation maps of MNE source reconstruction in the faces compared to the scrambled faces condition based on a t-test corrected for multiple comparison using False Discovery Rate (FDR). The color map illustrates the effect size with red indicating higher activity in the faces condition and blue showing higher activity in the scrambled faces condition. Please note that no amplitude or size thresholds were applied. The localization appears more focal on the ventral surface of the temporal pole using the age appropriate head model compared to the adult BEM. [Please click here to view a larger version of this figure.](#)



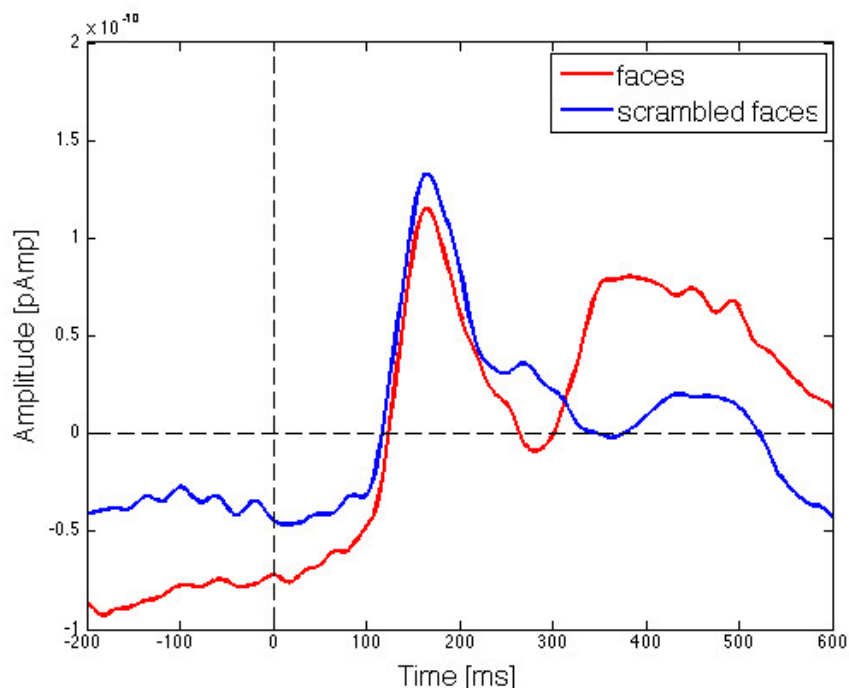


**Figure 7. Source ERP of the right fusiform gyrus in response to faces and scrambled faces based on source reconstruction of a recording obtained from a 6 year old boy (6 years 3 months) using an age appropriate BEM with MNE** The source ERP show a more negative deflection around 250 msec after stimulus onset in the faces condition compared to the scrambled faces condition. This activity is likely to reflect the contribution of the right fusiform gyrus to the N170 component in the faces condition.

Input for step 1.1	Description
<code>input_image = imread('/Users/some_user/images/example.jpeg');</code>	% Reading the image
<code>gray_image = rgb2gray(input_image);</code>	% Transferring from RGB to grey scale
<code>saveas(gray_image,'grey_image.tiff')</code>	% Save new image
Input for step 1.2	Description
Code Example:	
%%%	
% Housekeeping	
%%%	
<code>clc</code>	% clearing variables from workspace
<code>clear all</code>	
<code>close all</code>	% setting audio drivers to low latency mode
<code>InitializePsychSound([0]);</code>	
%%%	
% Variables	
%%%	
<code>input_folder = 'C:\Documents and Settings\ERP Lab Users\My Documents\MATLAB\Faces_Houses\';</code>	% defining the working directory
<code>netstation = 1;</code>	
	% this toggles communication with NetStation EEG recording software
	% defining the number of trials

no_of_trials = 80;	% unifying keyboard names for easy portability between Unix and PC versions
KbName('UnifyKeyNames')	% defining a variable for a escape key presses
escapeKey = KbName('ESCAPE');	
%%	
% Loading stimuli	
%%	
face_directory = strcat('C:\Documents and Settings\ERP Lab Users\My Documents\MATLAB\Faces_Houses\Faces\');	% supplying the folder with stimuli pictures
files = dir(face_directory);	% generating a list with all picture stimuli
faces = {files.name};	
faces(1:2) = [];	
grabbers = dir('/Users/joebathelt/Dropbox/preterm_oddball/grabbers/');	
grabbers = {grabbers.name};	
grabbers(1:2) = [];	
grabber_sounds = dir('/Users/joebathelt/Dropbox/preterm_oddball/sounds/');	
grabber_sounds = {grabber_sounds.name};	
grabber_sounds(1:2) = [];	
%%	
% Starting the experiment	
%%	
if netstation == 1; NetStation('Connect','194.82.245.131','55513')	% synchronisation with the recording software
NetStation('Synchronize',10)	% synchronisation within 10 msec of accuracy
NetStation('StartRecording')	% starts the recording
end	
% Setting up the screen	
screenNum=0;	% identification number of presentation screen
	% defining a window for stimulus presentation
[display.w, display.rect] = Screen('OpenWindow', screenNum, 0);	
[wPtr,rect]=Screen('OpenWindow',screenNum);	% hiding the mouse cursor
HideCursor;	
black=BlackIndex(wPtr);	% setting the background to black
Screen('FillRect',wPtr,black);	% defining font and font size for text display
Screen('TextFont', display.w, 'Arial');	
Screen('TextSize', display.w, 32);	
Screen('TextStyle',display.w, 0);	
for i=1:no_of_trials	
FlushEvents	
randomizer = randi(2);	
	% randomly selecting an attention grabber picture
attention_grabber = imread(strcat(input_folder,'grabbers/',cell2mat(grabbers(randi(length(grabbers))))));	
[sounds,fs,nbits] = wavread(strcat(input_folder,'sounds/',cell2mat(grabber_sounds(randi(length(grabber_sounds))))));	

audio_handle = PsychPortAudio('Open', [], [], 0, fs, length(sounds(1,:)));	
sounds = sounds';	% randomly selecting an attention grabber sound
PsychPortAudio('FillBuffer', audio_handle, sounds);	
	% setting up sound presentation
stimulus = strcat(face_directory,faces(randi(length(faces))));	
stimulus = imread(cell2mat(stimulus));	% this randomises the presentation of faces and scrambled faces
if randomizer == 2;	% loading the stimulus that was randomly selected from the list of stimuli
stimulus = stimulus(randperm(length(stimulus(:,1))),randperm(length(stimulus(1,:))));	
end	% scrambling the stimulus matrix, if the trial is a scrambled trial
stim=Screen('MakeTexture', wPtr, double(stimulus)); % stimulus	
	% preparing the stimulus for presentation
%%%	
% Trial	
%%%	
	% this section is only relevant to the first trial
if i == 1;	
[nx, ny, box] = DrawFormattedText(wPtr, 'Press any key to start', 'center', 'center',[255 255 255]);	
Screen('FrameRect', wPtr, 0, box);	
[VBLTimestamp StimulusOnsetTim] = Screen('Flip', wPtr);	% for the first trial, the text "Press any key to start" is presented until a key is pressed
KbWait([], 2);	
[nx, ny, box] = DrawFormattedText(display.w, ' ', 'center', 'center',255); % blank screen	
Screen('FrameRect', display.w, 0, box);	
[VBLTimestamp StimulusOnsetTim] = Screen('Flip', wPtr);	
end	
% Fixation Cross	
[nx, ny, bbox] = DrawFormattedText(wPtr, '+', 'center', 'center',255);	
Screen('FrameRect', display.w, 0, bbox);	
[VBLTimestamp StimulusOnsetTim] = Screen('Flip', wPtr);	% preparing a white plus sign in the centre of the screen as the fixation cross
if netstation == 1;	% presenting the fixation cross
NetStation('Event','fix+',StimulusOnsetTim) end	
	% sending a trigger with the time stamp of the fixation cross presentation and the code "fix+" to the EEG recording software
WaitSecs(0.15+rand*0.5)	% limiting presentation time of the fixation cross to a random duration between 0.15 and 0.2 sec
% Stimulus	% presenting the face or scrambled face stimulus
Screen('DrawTexture', wPtr, stim);	
[VBLTimestamp StimulusOnsetTim] = Screen(wPtr, 'Flip');	
if netstation == 1;	% sending trigger with time stamp and code 'face' or 'scra' face to EEG recording software
if randomizer == 1;	
NetStation('Event','face',StimulusOnsetTim)	
elseif randomizer == 2;	

NetStation('Event','scre',StimulusOnsetTim)	
end	
end	
WaitSecs(0.5)	% limit stimulus duration to 500 msec
	% presenting a blank screen
[nx, ny, box] = DrawFormattedText(wPtr, '', 'center', 'center',255); % blank screen	
Screen('FrameRect', wPtr, 0, box);	
[VBLTimestamp StimulusOnsetTim] = Screen('Flip',wPtr);	
WaitSecs(1+rand(1))	% inter trial interval with a random duration between 1 and 2 sec
% Attention grabber	% present the attention grabber with sound
Screen('DrawTexture', wPtr, grabber);	
sounds = PsychPortAudio('Start', audio_handle,15, 0, 1);	
[VBLTimestamp StimulusOnsetTim] = Screen('Flip',wPtr);	
if netstation == 1;	
NetStation('Event','grbr',StimulusOnsetTim)	% send the time stamp and code for the attention grabber to the EEG recording software
end	
	% present the attention grabber and sound until a key on the keyboard is pressed
KbWait([], 2);	
PsychPortAudio('Stop',audio_handle);	
Screen('FrameRect', display.w, 0, box);	% abort the experiment, if the escape key was pressed
[VBLTimestamp StimulusOnsetTim] = Screen('Flip',wPtr);	
[keyIsDown, timeSecs, keyCode ] = KbCheck; if keyIsDown	
if keyCode(escapeKey)	
disp('ESC')	
sca	
NetStation('StopRecording')	
return	
end	
end	% close the experiment and stop the EEG recording at the end of the experiment
end	
Screen('CloseAll');	
if netstation == 1;	
NetStation('StopRecording')	
end	
Input for step 3.1.1	Description
OUTEEG = pop_eegfilt(INEEG,0.1,[]);	% OUTEEG = EEG data after filtering, i.e. function output
	% INEEG = EEG data before filtering, i.e. function input
	% 0.1: high pass cut off frequency
	% []: low-pass cut-off, undefined because a high-pass filter is desired
Input for step 3.1.2	Description
OUTEEG = pop_eegfilt(INEEG,[],30);	% []: high pass cut off, undefined because a low pass filter is desired
	% 30: low-pass cut-off frequency
Input for step 3.1.3	Description

OUTEEG = pop_epoch(INEEG,'event',{'face','scra'},[-0.2 0.6]);	% Epoching
	% 'event',{'face','scra'}: the function is told to use the trigger events 'face' and 'scra' as the time locking markers. These triggers were defined in the experiment script to mark the onset of face and scrambled face stimulus presentation onset.
	% [-0.2 0.6] = time window for the ERP from 0.2 sec before the time-locking event to 0.6 sec
OUTEEG = pop_rmbase(EEG,[-0.2 0]);	% Removing the baseline
	% [-0.2 0]: baseline time window, i.e. 0.2 sec before the time-locking event to the time locking event
Input for step 3.1.4	Description
function [EEG] = threshold_rejection(EEG,threshold)	% function definition, the function requires an EEG dataset structure and a threshold in $\mu V$
for j=1:2	
for i = 1:length(EEG.data(1,1,:))	% this loops goes through all epochs in a given EEG data set
data = EEG.data(:,i);	
data = data - mean(data,2);	% subtracting the mean activity to avoid the influence of amplitude shifts
maxima = max(abs(data'));	% identifying the maximum absolute activity in all channels
bad_channels = maxima>threshold;	
channel_rejection(:,i) = bad_channels;	
if sum(bad_channels) > 0.2*128	% If more than 20% of channels are above the threshold, the epoch is marked for rejection
epoch_rejection(i) = 1;	
else	
epoch_rejection(i) = 0;	
end	
end	
if j==1;	% selecting only the epochs that are not marked as bad
EEG = pop_select(EEG,'trial',find(epoch_rejection==0))	
else	% mark channels that are bad in more than 20% of epochs after epoch rejection for channel rejection
bad_channels = mean(channel_rejection,2)>0.2;	
EEG = pop_interp(EEG,find(bad_channels == 1),'spherical');	% apply spherical interpolation to bad channels
end	
end	
Input for step 3.1.5	Description
EEG = pop_reref(EEG,[]);	% calculates the average reference
Input for step 3.2.1	Description
channels = {'E84', 'E89', 'E90', 'E91', 'E94','E95','E96'}; % right N170	% Occipito-temporal channels of the right hemisphere % for N170 responses using the channel labels for the % 128 channels Geodesic Hydrocel Sensor Net
EEG = pop_select( EEG,'channel',channels);	% Selecting the channels
Virtual_channel = mean(EEG.data,1);	% Combining the individual channels to a virtual channel
Input for step 3.3.2	Description
N170_peak = max(abs((averaged_ERPs(0.13*srate+0.2*srate:0.2*srate+0.2*srate),[],2)));	% Maximum amplitude within a latency window for each participant in $\mu V$
N170_peaklatency = 1000*(find(averaged_ERP(0.13*srate+0.2*srate:0.2*srate+0.2*srate) == N170_peak) + 0.2*EEG.srate + 0.13 EEG.srate)./EEG.srate	% Peak latency in msec



N170_mean = mean(averaged_ERPs;.0.13*srate+0.2*srate:0.2*srate+0.2*srate),[],2);	% Mean amplitude in $\mu\text{V}$
--	-----------------------------------

**Table 1. MATLAB commands to implement the example experiment and analyze high-density EEG recordings on channel- and source-level.** The table summarizes the code to implement the faces vs scrambled faces example experiment. Further, the code for pre processing the raw EEG is presented. In addition, methods for extracting waveform characteristics for channel level analysis of the event-related response are shown.

## Discussion

The present article describes the recording and analysis of high density EEG for reconstruction of cortical generators using boundary element models based on age appropriate average MRI templates and depth weighted minimum norm estimation in a standard ERP paradigm suitable for children. In this paradigm, pictures of faces and scrambled faces are presented. Different authors used this paradigm to investigate the development of face processing mechanisms over development<sup>35</sup>. On the channel level, more negative deflections over right occipito temporal channels are described for the face condition to the scrambled face condition. The topography, latency and response characteristic are consistent with the N170 component<sup>34</sup>. Previous source and simultaneous EEG fMRI investigations report that the fusiform gyrus is a likely generator of the N170 response. The results of the current analysis show that source inversion with a depth weighted boundary element model (BEM) can be used to localize source activity in the fusiform gyrus in the face scrambled face paradigm on the level of individual participants. The use of head models based on the individual participant's anatomy or the use of age appropriate averaged anatomical scans for developmental studies, in which the individual anatomy is not available, will allow the most accurate source localization<sup>2</sup>. Further, regions of interest can be identified based on anatomical knowledge or automatic parcellation algorithms to investigate the event related response of particular cortical regions.

There are several limitations to source reconstruction, particularly in developmental samples, at the moment. First, source reconstruction based on average templates for different age groups assumes that the individual shows typical brain development for their chronological age, which might not necessarily be the case, especially in patient groups. For example, various studies described atypical trajectories in brain growth for children born preterm<sup>36</sup> or children with autism<sup>37</sup>. It is hard to estimate how these anatomical differences will influence the accuracy of the inverse solution and bias results of comparisons between atypical and typical control groups.

Second, forward models such as the boundary element model (BEM) do not incorporate conductivity inhomogeneities within compartments, e.g., differences between grey and white matter. The accuracy for subcortical sources is therefore limited. Source solutions were restricted to cortical sources for that reason. Finite element models may be applied for more accurate resolution of subcortical generators. With solutions restricted to the cortex, it is important to keep in mind that activation in cortical regions may reflect underlying subcortical causative mechanisms, e.g., feedback communication via thalamic loops. Therefore, causal inferences about the involvement of cortical regions are limited unless more complex models are used that are currently only available for typical adult anatomy, e.g., Dynamic Causal Modelling<sup>38,39</sup>.

Further, Boundary element models assume closed shells for each compartment. However, young infants have soft spots in their skulls, where the sutures between the cranial bones are not fully merged<sup>15</sup>. This violation of BEM assumptions severely limits the applicability of source reconstruction with BEMs in infants younger than 2 years of age. Finite element models may be used for source reconstruction in this age range.

Third, even though age appropriate head models were used for source reconstruction, conductivity values based on adult samples were used to model conductivity within each compartment. However, tissue conductivity is likely to change over development, e.g., through increases in bone density<sup>15</sup>. Conductivity values for tissue types used in BEMs for human infants and children are currently not available to our knowledge.

## Disclosures

Publication costs for this article were sponsored by Electrical Geodesics, Inc.

## Acknowledgements

We want to thank Prof. John Richards, University of South Carolina, for granting us access to the Developmental MRI database and helpful discussions. We would also like to thank our funders Great Ormond Street Children's Charity, UCL Impact & Grand Challenges.

## References

1. Michel, C. M., & Murray, M. M. Towards the utilization of EEG as a brain imaging tool. *NeuroImage*. **61** (2), 371–385, doi:10.1016/j.neuroimage.2011.12.039 (2012).
2. Brodbeck, V. *et al.* EEG microstates of wakefulness and NREM sleep. *NeuroImage*. **62** (3), 2129–2139, doi:10.1016/j.neuroimage.2012.05.060 (2012).
3. Sanchez, C. E., Richards, J. E., & Almlí, C. R. Age-specific MRI templates for pediatric neuroimaging. *Developmental Neuropsychology*. **37** (5), 379–399, doi:10.1080/87565641.2012.688900 (2012).
4. Umutlu, L., Ladd, M. E., Forsting, M., & Lauenstein, T. 7 Tesla MR Imaging: Opportunities and Challenges. *RoFo : Fortschritte auf dem Gebiete der Röntgenstrahlen und der Nuklearmedizin*. **186** (2), 121–129, doi:10.1055/s-0033-1350406 (2014).
5. Logothetis, N. K. Bold claims for optogenetics. *Nature*. **468** (7323), E3–E4, doi:10.1038/nature09532 (2010).
6. Logothetis, N. K. What we can do and what we cannot do with fMRI. *Nature*. **453** (7197), 869–878, doi:10.1038/nature06976 (2008).
7. Roche-Labarbe, N. *et al.* High-resolution electroencephalography and source localization in neonates. *Human Brain Mapping*. **29** (2), 167–176, doi:10.1002/hbm.20376 (2008).

8. Johnson, M. H. Interactive Specialization: A domain-general framework for human functional brain development? *Developmental cognitive neuroscience*. **1**, 7–21, doi:10.1016/j.dcn.2010.07.003 (2010).
9. Nelson, C. A., & McCleery, J. P. Use of Event-Related Potentials in the Study of Typical and Atypical Development. *Journal of the American Academy of Child & Adolescent Psychiatry*. **47** (11), 1252–1261, doi:10.1097/CHI.0b013e318185a6d8 (2008).
10. Michel, C. M., Murray, M. M., Lantz, G., Gonzalez, S., Spinelli, L., & Grave de Peralta, R. EEG source imaging. *Clinical neurophysiology : official journal of the International Federation of Clinical Neurophysiology*. **115** (10), 2195–2222, doi:10.1016/j.clinph.2004.06.001 (2004).
11. Bathelt, J., O'Reilly, H., Clayden, J. D., Cross, J. H., & de Haan, M. Functional brain network organisation of children between 2 and 5 years derived from reconstructed activity of cortical sources of high-density EEG recordings. *NeuroImage*. **82**, 595–604, doi:10.1016/j.neuroimage.2013.06.003 (2013).
12. David, O., Cosmelli, D., & Friston, K. J. Evaluation of different measures of functional connectivity using a neural mass model. *NeuroImage*. **21** (2), 659–673, doi:10.1016/j.neuroimage.2003.10.006 (2004).
13. Grech, R. *et al.* Review on solving the inverse problem in EEG source analysis. *Journal of NeuroEngineering and Rehabilitation*. **5** (1), 25, doi:10.1186/1743-0003-5-25 (2008).
14. Wendel, K. *et al.* EEG/MEG source imaging: methods, challenges, and open issues. *Computational Intelligence and Neuroscience*. **2009**, 13, doi:10.1155/2009/656092 (2009).
15. Richards, J. E. Localizing cortical sources of event-related potentials in infants' covert orienting. *Developmental Science*. **8** (3), 255–278, doi:10.1111/j.1467-7687.2005.00414.x (2005).
16. Hauk, O. Keep it simple: a case for using classical minimum norm estimation in the analysis of EEG and MEG data. *NeuroImage*. **21** (4), 1612–1621, doi:10.1016/j.neuroimage.2003.12.018 (2004).
17. Pascual-Marqui, R. D. *et al.* Low resolution brain electromagnetic tomography (LORETA) functional imaging in acute, neuroleptic-naive, first-episode, productive schizophrenia. *Psychiatry Research*. **90** (3), 169–179 (1999).
18. Pascual-Marqui, R. D. Standardized low-resolution brain electromagnetic tomography (sLORETA): technical details. *Methods and findings in experimental and clinical pharmacology*. **24 Suppl D** (SUPPL. D), 5–12 (2002).
19. Phillips, C., Rugg, M. D., & Friston, K. J. Systematic regularization of linear inverse solutions of the EEG source localization problem. *NeuroImage*. **17** (1), 287–301, doi:10.1006/nimg.2002.1175 (2002).
20. Yao, J., & Dewald, J. P. A. Evaluation of different cortical source localization methods using simulated and experimental EEG data. *NeuroImage*. **25** (2), 369–382, doi:10.1016/j.neuroimage.2004.11.036 (2005).
21. Tandonnet, C., Burle, B., Hasbroucq, T., & Vidal, F. Spatial enhancement of EEG traces by surface Laplacian estimation: Comparison between local and global methods. *Clinical Neurophysiology*. **116** (1), 18–24, doi:10.1016/j.clinph.2004.07.021 (2005).
22. Tenke, C. E., & Kayser, J. Generator localization by current source density (CSD): implications of volume conduction and field closure at intracranial and scalp resolutions. *Clinical neurophysiology : official journal of the International Federation of Clinical Neurophysiology*. **123** (12), 2328–2345, doi:10.1016/j.clinph.2012.06.005 (2012).
23. Brainard, D. H. The psychophysics toolbox. *Spatial vision*, doi:10.1163/156856897X00357 (1997).
24. Kleiner, M., Brainard, D., Pelli, D., Ingling, A., & Murray, R. What's new in Psychtoolbox-3. *Perception*. (2007).
25. Tottenham, N. *et al.* The NimStim set of facial expressions: judgments from untrained research participants. *Psychiatry Research*. **168** (3), 242–249, doi:10.1016/j.psychres.2008.05.006 (2009).
26. Chaste, P. *et al.* Adjusting head circumference for covariates in autism: Clinical correlates of a highly heritable continuous trait. *Biological Psychiatry*. **74** (8), 576–584, doi:10.1016/j.biopsych.2013.04.018 (2013).
27. Delorme, A. *et al.* EEGLAB, SIFT, NIFT, BCILAB, and ERICA: New tools for advanced EEG processing. *Computational Intelligence and Neuroscience*. **2011**, 130714, doi:10.1155/2011/130714 (2011).
28. Nolan, H., Whelan, R., & Reilly, R. B. FASTER: Fully Automated Statistical Thresholding for EEG artifact Rejection. *Journal of Neuroscience Methods*. **192** (1), 152–162, doi:10.1016/j.jneumeth.2010.07.015 (2010).
29. Kilner, J. M. Bias in a common EEG and MEG statistical analysis and how to avoid it. *Clinical Neurophysiology*, doi:10.1016/j.clinph.2013.03.024 (2013).
30. DeBoer, T., Scott, L. S., & Nelson, C. A. 12 ERPs in Developmental Populations. *Event-related Potentials: A ....* (2005).
31. Sanchez, C. E., Richards, J. E., & Almli, C. R. Neurodevelopmental MRI brain templates for children from 2 weeks to 4 years of age. *Developmental Psychobiology*. **54** (1), 77–91, doi:10.1002/dev.20579 (2011).
32. Tadel, F., Baillet, S., Mosher, J. C., Pantazis, D., & Leahy, R. M. Brainstorm: A user-friendly application for MEG/EEG analysis. *Computational Intelligence and Neuroscience*. **2011**, 879716, doi:10.1155/2011/879716 (2011).
33. Haan, M., Johnson, M. H., & Halit, H. Development of face-sensitive event-related potentials during infancy: a review. *International Journal of Psychophysiology*. **51** (1), 45–58, doi:10.1016/S0167-8760(03)00152-1 (2003).
34. Earp, B. D., & Everett, J. A. C. Is the N170 face specific? Controversy, context, and theory. *Neuropsychological Trends*. **13** (1), 7–26, doi:10.1162/jocn.2007.19.3.543 (2013).
35. Taylor, M. J., McCarthy, G., Saliba, E., & Degiovanni, E. ERP evidence of developmental changes in processing of faces. *Clinical neurophysiology : official journal of the International Federation of Clinical Neurophysiology*. **110** (5), 910–915, doi:10.1016/S1388-2457(99)00006-1 (1999).
36. Ment, L. R. *et al.* Longitudinal brain volume changes in preterm and term control subjects during late childhood and adolescence. *PEDIATRICS*. **123** (2), 503–511, doi:10.1542/peds.2008-0025 (2009).
37. Courchesne, E. *et al.* Impairment in shifting attention in autistic and cerebellar patients. *Behavioral Neuroscience*. **108** (5), 848–865 (1994).
38. Litvak, V. *et al.* EEG and MEG data analysis in SPM8. *Computational Intelligence and Neuroscience*. **2011**, 852961, doi:10.1155/2011/852961 (2011).
39. Daunizeau, J., David, O., & Stephan, K. E. Dynamic causal modelling: A critical review of the biophysical and statistical foundations. *NeuroImage*. **58** (2), 312–322, doi:10.1016/j.neuroimage.2009.11.062 (2011).